low-temperature spectra using our standard technique. However, with the INEPT pulse sequence, we have acquired spectra (Figure 4) at −40 °C in $CD_2Cl_2/C_6D_6$ (80:20). At this temperature, both resonances sharpened considerably and the intensity 2 resonance split into a doublet ($J_{Y-Si}$ = 7.7 Hz). The other resonance showed no sign of coupling. This unambiguously identifies the upfield resonance as resulting from the terminal siloxides, as the large Y–O–Si angles should favor a large Y/Si coupling constant. The bridging siloxides have relatively small Y–O–Si angles (142 and 111°), and a correspondingly small Y/Si coupling is expected.

## Conclusions

The results presented here are perhaps the most interesting when they involve aggregated species containing inequivalent yttrium (or silicon) sites. This is because detection of rearrangement of metal polyhedra almost demands direct observation of metal NMR spectra. However, the detection of intra- and intermolecular exchange of siloxide ligands has also been demonstrated by $^{29}Si$ NMR spectroscopy. Chemical-shift-based discrimination between bridging and terminal siloxide groups appears promising. In addition, studies of complexes that contain $\mu_3$-$OSiR_3$ groups[2] indicate that these ligands may also be uniquely identified via $^{29}Si$ NMR spectroscopy.

**Acknowledgment.** Michael McGeary and Olivier Poncelet are acknowledged for contributions at the genesis of this project. We thank Frank Feher, Ted Budzichowski, Robert Addleman, and Deon Osman for assistance at critical times during this work and the U.S. Department of Energy for financial support.

**Registry No.** I, 118458-20-1; III, 128683-45-4; $^iPrOH$, 67-63-0; $CH_2Cl_2$, 75-09-2; $C_6D_6$, 1076-43-3; $HOCH_2CH_2OMe$, 109-86-4; $[Y(OCH_2CH_2OMe)_3]_{10}$, 126939-63-7; $Y(OSiPh_3)_3(OPBu_3)_2$, 133270-51-6; $Y(OSiPh_3)_4(DME)^-$, 133270-54-9; $Y(OSiPh_3)_3(THF)_3$, 122020-72-8; $HOSiPh_3$, 791-31-1; $[Y(\mu\text{-}OSiPh_3)(OSiPh_3)_2]_2$, 135658-43-4; toluene, 108-88-3.

Contribution from the Department of Chemistry and Laboratory for Molecular Structure and Bonding, Texas A&M University, College Station, Texas 77843

# New Halogen-Bridged Dinuclear Edge-Sharing and Face-Sharing Bioctahedral Tungsten(III) Complexes, $W_2X_6(PR_3)_n$, Where X = Cl or Br, $PR_3$ = $PMe_3$, $PMe_2Ph$, or $PBu_3$, and *n* = 4 or 3: Crystal Structures of $W_2Cl_6(PMe_2Ph)_4$, $W_2Cl_6(PMe_2Ph)_3$, and $W_2Br_6(PMe_2Ph)_3$

F. Albert Cotton* and Sanjay K. Mandal

*Received September 20, 1991*

The reduction of $WCl_4$ by 1 equiv of reducing agent, either Na/Hg or $NaB(C_2H_5)_3H$, in toluene followed by the addition of 2 equiv (or an excess) of phosphine ligand produced the edge-sharing compound $W_2Cl_6(PMe_2Ph)_4$ (**1**) in high yield. The face-sharing compounds $W_2Cl_6(PMe_2Ph)_3$ (**2**) and $W_2Cl_6(PBu_3)_3$ (**3**) were prepared by reacting $WCl_4$ with 1 equiv of reducing agent (Na/Hg for **2** and $NaB(C_2H_5)_3H$ in THF for **3**) in toluene followed by the addition of 1.5 equiv of the appropriate phosphine ligand. The first bromo-bridged dinuclear complexes $W_2Br_6(PMe_2Ph)_3$ (**4a**) and $W_2Br_6(PMe_3)_3$ (**5**) were synthesized by reducing $WBr_5$ with 2 equiv of reducing agent (Na/Hg for **4a** and NaB $(C_2H_5)_3H$ in toluene for **5**) in toluene followed by the addition of 1.5 equiv of $PMe_2Ph$ and $PMe_3$, respectively. Compounds **1**, **2**, and **4a,b** have been structurally characterized by X-ray diffraction studies. Compound **4** (**4a,b**) exists in two different crystalline forms. Crystal data: for **1**, space group $C2/c$, $a$ = 17.577 (2) Å, $b$ = 11.200 (1) Å, $c$ = 21.001 (3) Å, $\beta$ = 108.25 (2)°, $V$ = 3934 (2) Å$^3$, and $Z$ = 4; for **2**, space group $P\bar{1}$, $a$ = 9.796 (2) Å, $b$ = 12.603 (2) Å, $c$ = 13.856 (3) Å, $\alpha$ = 76.51 (2)°, $\beta$ = 82.66 (2)°, $\gamma$ = 73.47 (1)°, $V$ = 1591 (1) Å$^3$, and $Z$ = 2; for **4a**, space group $P\bar{1}$, $a$ = 9.896 (3) Å, $b$ = 12.866 (4) Å, $c$ = 14.246 (3) Å, $\alpha$ = 75.62 (2)°, $\beta$ = 82.95 (2)°, $\gamma$ = 74.07 (2)°, $V$ = 1687 (1) Å$^3$, and $Z$ = 2; for **4b**, space group $P\bar{1}$, $a$ = 10.665 (2) Å, $b$ = 16.009 (5) Å, $c$ = 10.154 (3) Å, $\alpha$ = 98.12 (2)°, $\beta$ = 101.92 (2)°, $\gamma$ = 79.95 (2)°, $V$ = 1660 (1) Å$^3$, and $Z$ = 2. In all these complexes, the W–W bond distances 2.6950 (3) (**1**), 2.4433 (4) (**2**), 2.4768 (9) (**4a**), and 2.4496 (6) Å (**4b**) indicate strong metal–metal bonding. The face-sharing compounds **2** and **4b** have the shortest W–W bond distances in any neutral halogen-bridged dinuclear tungsten(III) complexes so far reported. The average W–$X_b$–W bond angle in the edge-sharing compound **1** is 68.98 (3)° and those in the face-sharing compounds are 58.45 [4], 56.28 [3], and 55.32 [2]° for **2**, **4a**, and **4b** respectively. Compounds **3** and **5** have been characterized by a $^{31}P\{^1H\}$ NMR spectrum and an electronic spectrum (similar to that of **4**), respectively.

## Introduction

The chemistry of dinuclear transition metal complexes containing direct metal–metal bonds has been of great interest for over 3 decades.[1] One of the most interesting subsets of this family is the one having the general formula $M_2L_n^{m-}$, where M = transition metal, $L_n$ represents an assembly of halogen atoms and monodentate neutral ligands, $n$ = 9 or 10, and the value of $m$ depends on the transition metal as well as its oxidation state and the number of neutral ligand present in the molecule. When $n$ = 9, these complexes adopt the face-sharing bioctahedral geometry (type I) while complexes with $n$ = 10 have the edge-sharing bioctahedral geometry (type II). Type I complexes with three and type II complexes with four monodentate phosphine ligands in the terminal positions may have different ligand arrangements among the terminal halogen and phosphorus atoms for different transition metals.[2] Such complexes of group 6 metals have attracted much attention recently due to their interesting structural features and chemical properties. Studies on chromium compounds[3] show that there is never any direct metal–metal bonding in these complexes. Extensive studies on molybdenum compounds[4–6] have been reported in the literature, and it is found that a direct metal–metal bond is present in all complexes except

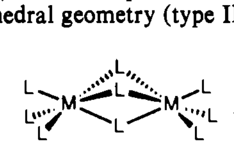


I

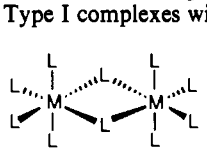


II

* Author to whom correspondence should be directed.

(1) (a) Cotton, F. A.; Walton, R. A. *Multiple Bonds Between Metal Atoms*; Wiley: New York, 1982. (b) Cotton, F. A. *Acc. Chem. Res.* **1978**, *11*, 225. (c) Cotton, F. A.; Chisholm, M. H. *Chem. Eng. News* **1982**, *60*, 40. (d) Cotton, F. A. *J. Chem. Educ.* **1983**, *60*, 713. (e) Cotton, F. A.; Walton, R. A. *Struc. Bonding (Berlin)* **1985**, *62*, 1.
(2) (a) Messerle, L. *Chem. Rev.* **1988**, *88*, 1229. (b) Cotton, F. A.; Shang, M.; Wojtczak, W. A. *Inorg. Chem.* **1991**, *30*, 3670 and references therein.
(3) Cotton, F. A.; Eglin, J. L.; Luck, R. L.; Son, K-A. *Inorg. Chem.* **1990**, *29*, 1802.
(4) Mui, H. D.; Poli, R. *Inorg. Chem.* **1989**, *28*, 3609.
(5) Cotton, F. A.; Luck, R. L.; Son, K-A. *Inorg. Chim. Acta* **1990**, *173*, 131.
(6) Poli, R.; Mui, H. D. *Inorg. Chem.* **1991**, *30*, 65.

 

$Mo_2Cl_6(PEt_3)_4$. On the other hand, similar compounds of tungsten have been reported only in a preliminary form by Chisholm et al.[7] We carried out this research to extend the chemistry of tungsten by developing new synthetic methods for the preparation of these complexes, as well as by characterizing them structurally and with other physical methods. In this report we describe new synthetic methods starting from $WCl_4$ for the preparation of chloro-bridged edge-sharing and face-sharing complexes of W(III) with different phosphine ligands using two different reducing agents. We also report the synthesis of the first bromo-bridged dinuclear complexes of W(III) and the structural characterization of the first bromo-bridged dinuclear complex $W_2Br_6(PMe_2Ph)_3$.

## Experimental Section

**Materials and Methods.** All manipulations were carried out under an atmosphere of argon by employing standard vacuum line and Schlenk techniques.[8] All solvents were predried over 8–12 mesh molecular sieves (pore size: 3 or 4 Å) and freshly distilled from appropriate drying agents under an atmosphere of dinitrogen prior to use. Chemicals were obtained from the following sources: $PMe_3$, $PBu_3$, and $PMe_2Ph$, Strem Chemical Co.; $WCl_4$, $WBr_5$, and 1 M $NaB(C_2H_5)_3H$ in THF or in toluene, Aldrich Chemical Co. Solid chemicals were used as received in a drybox. Liquid chemicals (as received) were transferred into separate Schlenk tubes under an atmosphere of argon and were stored in the refrigerator when not used. Triple-distilled grade Hg, D. F. Goldsmith Chemical and Metal Corp., and Na metal, J. T. Baker Chem. Co., were used as received. Sodium amalgam was prepared by dissolving a weighed amount of metallic sodium in an approximately measured quantity of Hg that was pumped under vacuum for at least an hour in a three-neck flask inside a drybox. Reducing agents and phosphine ligands were introduced to the reaction vessels with the help of a syringe which was prewashed with the solvent used in the reactions.

**Physical Measurements.** Electronic spectra were recorded by using toluene solutions in quartz cells on a Cary 17 UV–vis spectrophotometer.

**NMR Spectra.** The $^{31}P\{^1H\}$ NMR spectrum of **3** in toluene was run on a Varian XL-200 spectrometer in a tube containing a sufficient amount of $C_6D_6$. The $^{31}P$ shifts (in ppm) were reported relative to external 85% (aqueous) $H_3PO_4$, measured immediately before and after the spectrum was recorded.

**Syntheses. $W_2X_6(PR_3)_4$ Complexes. $W_2Cl_6(PMe_2Ph)_4$ (1).** To a three-neck flask charged with $WCl_4$ (1 mmol, 325 mg) was added 25 mL of toluene, and a slurry was formed upon stirring. A 1-mL aliquot of 1 M $NaB(C_2H_5)_3H$ in THF or 0.5 mL of 2 M Na/Hg was introduced to this flask with the help of a syringe, and the mixture was stirred for 10–20 min. A deep green solution was obtained, and to this solution was added 0.30 mL (2 mmol) or an excess of $PMe_2Ph$. After stirring it for a further 2 d, the dark solution was filtered through Celite. The solution was then layered with hexane, and a crop of dark red crystals was obtained in 3 d. These crystals were used for other studies including X-ray crystallography. Isolated yields: 50–75%. UV–vis spectrum (toluene solution), nm: 670, 460, 370 (shoulder).

**$W_2X_6(PR_3)_3$ Complexes. (i) $W_2Cl_6(PMe_2Ph)_3$ (2).** To a slurry of $WCl_4$ (1 mmol, 325 mg) in 30 mL of toluene in a three-neck flask was introduced 0.5 mL of 2 M Na/Hg by syringe. A deep green solution was obtained after stirring for 30 min, and to this solution was added 0.22 mL (1.5 mmol) of $PMe_2Ph$. This mixture was stirred at room temperature for 1 d, giving a red solution, which was filtered through Celite. The red filtrate was layered carefully with hexane. Crystals were harvested after 3 weeks. Yield: 60% based on $WCl_4$.

**(ii) $W_2Cl_6(PBu_3)_3$ (3).** To a three-neck flask containing $WCl_4$ (1 mmol, 325 mg) was added 25 mL of toluene. A 1-mL aliquot of 1 M $NaB(C_2H_5)_3H$ in THF was introduced by syringe, and the mixture was stirred for 20 min. A deep green solution was obtained and to this solution was added 0.38 mL (1.5 mmol) of $PBu_3$. After it had been stirred for 2 d, the red-brown solution was filtered from the undissolved black residue through Celite, and the red-brown filtrate was layered with hexane. Unfortunately, no crystal suitable for X-ray diffraction work was found. $^{31}P\{^1H\}$ NMR spectrum of this solution: a doublet at $\delta = -33.71$ ppm and a triplet at $\delta = 20.84$ ppm (2:1 ratio) and $J_{P-P} = 44.7$ Hz.

**(iii) $W_2Br_6(PMe_2Ph)_3$ (4a).** To a suspension of $WBr_5$ (584 mg, 1.0 mmol) in 30 mL of toluene was introduced 1 mL of 2 M Na/Hg by syringe. The mixture was stirred for $^1/_2$ h, and 0.22 mL (1.5 mmol) of $PMe_2Ph$ was then added to it. The stirring was continued for 2 d. A brown solid was separated from a red-brown solution by filtration under an atmosphere of argon. The brown solid was dissolved in methanol, and the solution was kept in a refrigerator. Purple crystals which formed within 3 d were found to be $WOBr_2(PMe_2Ph)_3 \cdot 0.5C_7H_8$.[9] The red-brown solution was layered with hexane and afforded red crystals over a period of 3 weeks. One of these crystals was used for X-ray diffraction studies. The yield of this compound was ca. 35% with respect to $WBr_5$. UV–vis spectrum (toluene solution), nm: 690, 490.

When this method was repeated with careful elimination of oxygen, no oxo product was obtained and the yield was ca. 70%. This compound can also be prepared by using $NaB(C_2H_5)_3H$ as reducing agent instead of Na/Hg in the above procedure (checked by UV–vis spectroscopy). Another crystalline form of the compound, **4b**, was fortuitously obtained from a toluene and $C_6D_6$ mixture in a $^{31}P$ NMR tube, but we have not been able to obtain such crystals again.

**(iv) $W_2Br_6(PMe_3)_3$ (5).** A 2-mL aliquot of 1 M $NaB(C_2H_5)_3H$ in toluene was added to a three-neck flask containing 1 mmol of $WBr_5$ (584 mg) in 30 mL of toluene. After $^1/_2$ h of stirring, 0.14 mL (1.5 mmol) of $PMe_3$ was added and stirring was continued for 2 d. A red-brown solution was filtered from the undissolved residue through Celite. Hexane was added to the filtrate to precipitate it completely. Isolated yield: 30%. UV–vis spectrum (toluene solution), nm: 680, 490. Several attempts to get suitable single crystals for X-ray diffraction studies failed.

**X-ray Crystallography.** In each case a crystal of suitable size and quality was mounted on the tip of a thin glass fiber with the use of epoxy cement. X-ray diffraction experiments were carried out using one of two fully automated four-circle diffractometers, Nicolet P3 and Rigaku AFC5R. These diffractometers were equipped with monochromated Mo Kα radiation (λ = 0.710 73 Å) or monochromated Cu Kα radiation (λ = 1.540 598 Å), respectively. Unit cell determination and data collection followed routine procedures and practices of this laboratory.[10] Oscillation photographs of principal axes were taken to confirm the Laue class, symmetry, and the axial lengths as well as to evaluate crystal quality. *C*-Centering of **1** was verified by taking photographs of the *ab* face. During each data collection, three intensity standards were collected periodically to check the crystal decay, and an appropriate correction was made to the data for the decay. At the end of data collection azimuthal ($\psi$) scans were done on several reflections having Eulerian angles $\chi = 90 \pm 10$ or $270 \pm 10°$. The average of the $\psi$ scans was the basis for the empirical absorption corrections applied to the data sets.[11] All data were also corrected for Lorentz and polarization effects.

The structures were solved and refined using the SHELXS-86[12] and the VAX-SDP[13] programs. Crystallographic parameters and structure refinement data for all structures reported here are listed in Tables I and II.

**Crystal Structure of 1.** The $\omega$–$2\theta$ scan technique was used to scan data points over an octant of reciprocal space. There was no significant decay of the crystal as indicated by the intensity standards. The monoclinic space group $C2/c$ was chosen to start the refinement of the structure and was proved to be correct through successful refinement. Positions of all atoms heavier than carbon were obtained from a Patterson synthesis, and the remainder of the molecule was located and refined by alternating difference Fourier maps and least-squares cycles. Anisotropic displacement parameters were assigned to all atoms of the neutral molecule. Hydrogen atoms were introduced at calculated positions and used for the structure factor calculations but not refined. The final Fourier map did not have any significant peak. The final positional and thermal parameters of the non-hydrogen atoms for this structure are listed in Table III, and those of the hydrogen atoms are available in the supplementary material.

**Crystal Structure of 2.** Data were collected in the triclinic crystal system. Three intensity standards showed no significant change in intensities during the 96.8 h of exposure to X-rays. Since this compound was crystallographically isomorphous with **4a**, atomic coordinates of tungsten atoms were taken from **4a**, which had been solved earlier, to initiate the refinement. The remainder of the molecule was located and refined by alternating difference Fourier maps and least-squares cycles. Anisotropic displacement parameters were assigned to all atoms. Hydrogen atoms were included in the model at calculated positions to calculate the structure factors but not refined. The final difference Fourier map had three peaks greater than 1 e/Å$^3$ (highest 2.041 e/Å$^3$) but all

(7) Chacon, S. T.; Chisholm, M. H.; Strieb, W. E.; William, V. D. S. *Inorg. Chem.* **1989**, *28*, 5.
(8) Shriver, D. F.; Drezden, M. A. *The Manipulation of Air Sensitive Compounds*, 2nd ed., Wiley: New York, 1986.
(9) Cotton, F. A.; Mandal, S. K. *Inorg. Chim. Acta*, in press.
(10) (a) Bino, A.; Cotton, F. A.; Fanwick, P. E. *Inorg. Chem.* **1979**, *18*, 3558. (b) Cotton, F. A.; Frenz, B. A.; Deganello, G.; Shaver, A. J. *J. Organomet. Chem.* **1973**, *50*, 227.
(11) North, A. C. T.; Phillips, D. C.; Mathews, F. S. *Acta Crystallogr., Sect. A: Cryst. Phys., Diffr., Theor. Gen. Crystallogr.* **1968**, *24*, 351.
(12) Sheldrick, G. M. SHELXS-86. Institut fur Anorganische Chemie der Universitat, Göttingen, FRG, 1986.
(13) SDP/V V3.0 Package of Programs. Frenz, B. A. and Associates, Inc., College Station, TX, 1985.

**Table I.** Crystal Data for $W_2Cl_6(PMe_2Ph)_4$ (**1**) and $W_2Cl_6(PMe_2Ph)_3$ (**2**)

| | **1** | **2** |
|---|---|---|
| formula | $C_{32}H_{44}Cl_6P_4W_2$ | $C_{24}H_{33}Cl_6P_3W_2$ |
| fw | 1133.022 | 994.87 |
| space group | $C2/c$ (No. 15) | $P\bar{1}$ (No. 2) |
| syst abs | $hkl$, $h + k \neq 2n$<br>$h0l$, $l \neq 2n$ | |
| $a$, Å | 17.577 (2) | 9.796 (2) |
| $b$, Å | 11.220 (1) | 12.603 (2) |
| $c$, Å | 21.001 (3) | 13.856 (3) |
| $\alpha$, deg | | 76.51 (2) |
| $\beta$, deg | 108.25 (2) | 82.66 (2) |
| $\gamma$, deg | | 73.47 (1) |
| $V$, Å$^3$ | 3934 (2) | 1591 (1) |
| $Z$ | 4 | 2 |
| $d_{calc}$, g/cm$^3$ | 1.913 | 2.076 |
| cryst size, mm | 0.70 × 0.30 × 0.20 | 0.50 × 0.15 × 0.04 |
| $\mu$(Mo K$\alpha$), cm$^{-1}$ | 65.67 | 80.54 |
| instrum used | Nicolet P3 | Nicolet P3 |
| radiation used; $\lambda$, Å | Mo K$\alpha$; 0.71073 | |
| temp, °C | 20 ± 1 | 20 ± 1 |
| scan method | $\omega$–$2\theta$ | $\omega$–$2\theta$ |
| data collcn $2\theta$ limits, deg | 4–50 | 4–50 |
| no. of unique data; no. with $F_o^2 > 3\sigma(F_o^2)$ | 3410; 3076 | 3864; 3795 |
| no. of params refined | 200 | 316 |
| transm factors, %: max; min | 99.73; 47.54 | 99.84; 55.66 |
| $R^a$ | 0.0231 | 0.0276 |
| $R_w{}^b$ | 0.0405 | 0.0355 |
| quality-of-fit$^c$ | 1.305 | 0.856 |
| largest shift/esd, final cycle | 0.01 | 0.09 |
| largest peak, e/Å$^3$ | 0.487 | 2.041 |

[a] $R = \sum||F_o| - |F_c||/\sum|F_o|$. [b] $R_w = [\sum w(|F_o| - |F_c|)^2/\sum w|F_o|^2]^{1/2}$; $w = 1/\sigma^2\{|F_o|\}$. [c] Quality-of-fit $= [\sum w(|F_o| - |F_c|)^2/(N_{observns} - N_{params})]^{1/2}$.

**Table II.** Crystal Data for $W_2Br_6(PMe_2Ph)_3$ (**4**)

| | **4a** | **4b** |
|---|---|---|
| formula | $C_{24}H_{33}Br_6P_3W_2$ | $C_{24}H_{33}Br_6P_3W_2$ |
| fw | 1261.61 | 1261.61 |
| space group | $P\bar{1}$ (No. 2) | $P\bar{1}$ (No. 2) |
| $a$, Å | 9.896 (3) | 10.665 (2) |
| $b$, Å | 12.866 (4) | 16.009 (5) |
| $c$, Å | 14.246 (3) | 10.154 (3) |
| $\alpha$, deg | 75.62 (2) | 98.12 (2) |
| $\beta$, deg | 74.07 (2) | 79.95 (2) |
| $V$, Å$^3$ | 1687 (1) | 1660 (1) |
| $Z$ | 2 | 2 |
| $d_{calc}$, g/cm$^3$ | 2.484 | 2.523 |
| cryst size, mm | 0.27 × 0.12 × 0.04 | 0.20 × 0.10 × 0.05 |
| $\mu$(Cu K$\alpha$), cm$^{-1}$ | 225.29 | 228.86 |
| instrum used | Rigaku AFC5R | Rigaku AFC5R |
| radiation used; $\lambda$, Å | Cu K$\alpha$; 1.540598 | |
| temp, °C | 20 ± 1 | 20 ± 1 |
| scan method | $\omega$–$2\theta$ | $\omega$–$2\theta$ |
| data collcn $2\theta$ limits, deg | 4–120 | 4–120 |
| no. of unique data; no. with $F_o^2 > 3\sigma(F_o^2)$ | 5025; 4139 | 4934; 4322 |
| no. of params refined | 316 | 316 |
| transm factors, %: max; min | 100.00; 38.84 | 100.00; 43.68 |
| $R^a$ | 0.055 | 0.0418 |
| $R_w{}^b$ | 0.078 | 0.0640 |
| quality-of-fit$^c$ | 1.858 | 1.550 |
| largest shift/esd, final cycle | 0.03 | 0.03 |
| largest peak, e/Å$^3$ | 2.178 | 0.910 |

[a] $R - \sum||F_o| - |F_c||/\sum|F_o|$. [b] $R_w = [\sum w(|F_o| - |F_c|)^2/\sum w|F_o|^2]^{1/2}$; $w = 1/\sigma^2\{|F_o|\}$. [c] Quality-of-fit $= [\sum w(|F_o| - |F_c|)^2/(N_{observns} = N_{params})]^{1/2}$.

were in the vicinity of the central core of the molecule. The final positional and thermal parameters of the non-hydrogen atoms for this structure are listed in Table IV, and those of the hydrogen atoms are available as supplementary material.

**Table III.** Positional and Isotropic Equivalent Displacement Parameters[a] and Their Estimated Standard Deviations for $W_2Cl_6(PMe_2Ph)_4$ (**1**)

| atom | $x$ | $y$ | $z$ | $B$, Å$^2$ |
|---|---|---|---|---|
| W(1) | 0.000 | 0.10257 (2) | 0.250 | 2.008 (5) |
| W(2) | 0.000 | 0.34277 (2) | 0.250 | 1.793 (4) |
| Cl(1) | 0.05665 (7) | 0.21981 (9) | 0.34665 (6) | 2.57 (2) |
| Cl(2) | 0.06028 (7) | −0.0568 (1) | 0.32991 (7) | 3.67 (3) |
| Cl(3) | −0.13158 (6) | 0.3824 (1) | 0.25363 (6) | 3.15 (2) |
| P(1) | −0.12526 (7) | 0.0695 (1) | 0.28456 (6) | 2.60 (2) |
| P(2) | 0.04710 (7) | 0.5035 (1) | 0.34276 (6) | 2.81 (2) |
| C(1) | −0.2181 (3) | 0.1000 (5) | 0.2182 (3) | 3.9 (1) |
| C(2) | −0.1373 (3) | −0.0878 (5) | 0.3039 (3) | 4.1 (1) |
| C(3) | −0.1328 (3) | 0.1433 (4) | 0.3597 (2) | 3.1 (1) |
| C(4) | −0.1942 (3) | 0.2223 (4) | 0.3585 (3) | 4.1 (1) |
| C(5) | −0.1983 (4) | 0.2756 (5) | 0.4173 (4) | 5.7 (2) |
| C(6) | −0.1410 (5) | 0.2462 (7) | 0.4770 (3) | 6.7 (2) |
| C(7) | −0.0805 (5) | 0.1727 (8) | 0.4791 (3) | 6.5 (2) |
| C(8) | −0.0760 (3) | 0.1183 (6) | 0.4204 (3) | 4.4 (1) |
| C(9) | 0.0903 (4) | 0.6366 (5) | 0.3194 (3) | 4.7 (1) |
| C(10) | −0.0297 (3) | 0.5630 (6) | 0.3749 (3) | 5.5 (1) |
| C(11) | 0.1243 (3) | 0.4570 (4) | 0.4185 (2) | 2.9 (1) |
| C(12) | 0.1066 (3) | 0.4062 (6) | 0.4721 (3) | 4.2 (1) |
| C(13) | 0.1677 (4) | 0.3711 (7) | 0.5287 (3) | 6.1 (2) |
| C(14) | 0.2437 (4) | 0.3858 (7) | 0.5334 (4) | 6.5 (2) |
| C(15) | 0.2635 (4) | 0.4385 (7) | 0.4823 (4) | 6.3 (2) |
| C(16) | 0.2055 (3) | 0.4720 (5) | 0.4239 (3) | 4.4 (1) |

[a] Values for anisotropically refined atoms are given in the form of the equivalent isotropic displacement parameter defined as $(4/3)[a^2\beta_{11} + b^2\beta_{22} + c^2\beta_{33} + ab(\cos\gamma)\beta_{12} + ac(\cos\beta)\beta_{13} + bc(\cos\alpha)\beta_{23}]$.

**Table IV.** Positional and Isotropic Equivalent Displacement Parameters[a] and Their Estimated Standard Deviations for $W_2Cl_6(PMe_2Ph)_3$ (**2**)

| atom | $x$ | $y$ | $z$ | $B$, Å$^2$ |
|---|---|---|---|---|
| W(1) | 0.18838 (3) | −0.04282 (2) | 0.24860 (2) | 2.204 (5) |
| W(2) | 0.23476 (3) | 0.13859 (2) | 0.24512 (2) | 2.453 (6) |
| Cl(1) | 0.1115 (2) | 0.0404 (1) | 0.3969 (1) | 3.06 (4) |
| Cl(2) | 0.4387 (2) | −0.0232 (2) | 0.2119 (1) | 3.37 (4) |
| Cl(3) | 0.0805 (2) | 0.1296 (2) | 0.1199 (1) | 3.50 (4) |
| Cl(4) | 0.2430 (2) | −0.1459 (2) | 0.1191 (1) | 3.75 (4) |
| Cl(5) | 0.3859 (2) | 0.1605 (2) | 0.3553 (1) | 4.40 (4) |
| Cl(6) | 0.0550 (2) | 0.3016 (2) | 0.2702 (2) | 4.43 (5) |
| P(1) | −0.0641 (2) | −0.0631 (2) | 0.2593 (1) | 2.79 (4) |
| P(2) | 0.3037 (2) | −0.2075 (2) | 0.3837 (1) | 3.05 (4) |
| P(3) | 0.3594 (2) | 0.2365 (2) | 0.0947 (1) | 3.27 (4) |
| C(1) | −0.1316 (8) | −0.0399 (7) | 0.1371 (6) | 4.2 (2) |
| C(2) | −0.1982 (8) | 0.0365 (7) | 0.3202 (6) | 4.2 (2) |
| C(3) | −0.0862 (7) | −0.2018 (6) | 0.3182 (6) | 3.5 (2) |
| C(4) | −0.0209 (9) | −0.2910 (7) | 0.2689 (7) | 4.9 (2) |
| C(5) | −0.031 (1) | −0.3999 (8) | 0.3126 (9) | 6.3 (3) |
| C(6) | −0.104 (1) | −0.4188 (9) | 0.4039 (9) | 7.0 (3) |
| C(7) | −0.168 (1) | −0.3308 (9) | 0.4532 (9) | 6.5 (3) |
| C(8) | −0.1574 (9) | −0.2229 (8) | 0.4098 (7) | 4.9 (2) |
| C(9) | 0.4294 (9) | −0.1709 (7) | 0.4483 (6) | 4.6 (2) |
| C(10) | 0.1831 (9) | −0.2545 (8) | 0.4839 (6) | 4.5 (2) |
| C(11) | 0.4074 (8) | −0.3377 (6) | 0.3461 (5) | 3.4 (2) |
| C(12) | 0.541 (1) | −0.3444 (8) | 0.2965 (8) | 6.1 (3) |
| C(13) | 0.622 (1) | −0.442 (1) | 0.2694 (9) | 7.4 (3) |
| C(14) | 0.573 (1) | −0.5373 (8) | 0.2933 (8) | 6.5 (3) |
| C(15) | 0.444 (1) | −0.5333 (8) | 0.3397 (8) | 7.1 (3) |
| C(16) | 0.360 (1) | −0.4334 (8) | 0.3657 (8) | 5.9 (3) |
| C(17) | 0.5453 (9) | 0.2208 (7) | 0.1123 (7) | 4.8 (2) |
| C(18) | 0.368 (1) | 0.1832 (8) | −0.0183 (7) | 5.7 (2) |
| C(19) | 0.2879 (8) | 0.3883 (6) | 0.0610 (6) | 3.4 (2) |
| C(20) | 0.320 (1) | 0.4565 (8) | 0.1141 (8) | 6.6 (3) |
| C(21) | 0.270 (1) | 0.5709 (8) | 0.092 (1) | 7.4 (3) |
| C(22) | 0.187 (1) | 0.6217 (9) | 0.016 (1) | 6.8 (3) |
| C(23) | 0.151 (1) | 0.562 (1) | −0.0383 (9) | 7.6 (3) |
| C(24) | 0.203 (1) | 0.4411 (9) | −0.0164 (8) | 7.0 (3) |

[a] Values for anisotropically refined atoms are given in the form of the equivalent isotropic displacement parameter defined as $(4/3)[a^2\beta_{11} + b^2\beta_{22} + c^2\beta_{33} + ab(\cos\gamma)\beta_{12} + ac(\cos\beta)\beta_{13} + bc(\cos\alpha)\beta_{23}]$.

**Crystal Structure of 4a.** Three intensity standards were indicative of no significant crystal decay. Positions of tungsten and bromine atoms

**Table V.** Positional and Isotropic Equivalent Displacement Parameters[a] and Their Estimated Standard Deviations for $W_2Br_6(PMe_2Ph)_3$ (**4a**)

| atom | x | y | z | B, Å² |
|---|---|---|---|---|
| W(1) | 0.18786 (6) | −0.04345 (4) | 0.24664 (4) | 2.94 (1) |
| W(2) | 0.23976 (6) | 0.13539 (4) | 0.24245 (4) | 3.03 (1) |
| Br(1) | 0.1123 (1) | 0.0364 (1) | 0.39979 (9) | 3.79 (3) |
| Br(2) | 0.4505 (1) | −0.0290 (1) | 0.2074 (1) | 3.92 (3) |
| Br(3) | 0.0741 (2) | 0.1334 (1) | 0.1140 (1) | 4.16 (3) |
| Br(4) | 0.2386 (2) | −0.1516 (1) | 0.1150 (1) | 4.84 (3) |
| Br(5) | 0.4012 (2) | 0.1570 (1) | 0.3563 (1) | 4.93 (3) |
| Br(6) | 0.0558 (2) | 0.3072 (1) | 0.2693 (1) | 5.16 (4) |
| P(1) | −0.0637 (3) | −0.0642 (3) | 0.2587 (2) | 3.49 (7) |
| P(2) | 0.3053 (4) | −0.2119 (3) | 0.3804 (3) | 4.37 (8) |
| P(3) | 0.3636 (4) | 0.2356 (3) | 0.0953 (3) | 3.79 (7) |
| C(1) | −0.134 (1) | −0.047 (1) | 0.141 (1) | 4.7 (3) |
| C(2) | −0.195 (2) | 0.037 (1) | 0.314 (1) | 5.1 (4) |
| C(3) | −0.084 (1) | −0.201 (1) | 0.322 (1) | 4.5 (3) |
| C(4) | −0.025 (2) | −0.288 (1) | 0.278 (1) | 5.8 (4) |
| C(5) | −0.036 (2) | −0.397 (2) | 0.325 (2) | 7.8 (6) |
| C(6) | −0.112 (2) | −0.410 (2) | 0.416 (2) | 8.9 (6) |
| C(7) | −0.172 (2) | −0.324 (2) | 0.460 (2) | 6.9 (5) |
| C(8) | −0.158 (2) | −0.215 (1) | 0.412 (1) | 5.5 (4) |
| C(9) | 0.430 (2) | −0.179 (1) | 0.446 (1) | 5.2 (4) |
| C(10) | 0.186 (2) | −0.261 (2) | 0.479 (1) | 6.2 (5) |
| C(11) | 0.407 (2) | −0.339 (1) | 0.344 (1) | 5.1 (4) |
| C(12) | 0.542 (2) | −0.346 (1) | 0.301 (2) | 6.9 (5) |
| C(13) | 0.619 (2) | −0.441 (2) | 0.275 (2) | 8.8 (6) |
| C(14) | 0.569 (2) | −0.535 (2) | 0.291 (1) | 7.4 (5) |
| C(15) | 0.434 (3) | −0.531 (2) | 0.335 (2) | 9.9 (7) |
| C(16) | 0.349 (2) | −0.431 (2) | 0.360 (2) | 7.3 (5) |
| C(17) | 0.548 (1) | 0.225 (1) | 0.112 (1) | 4.8 (4) |
| C(18) | 0.371 (2) | 0.189 (1) | −0.017 (1) | 6.2 (4) |
| C(19) | 0.290 (2) | 0.386 (1) | 0.062 (1) | 4.6 (3) |
| C(20) | 0.316 (2) | 0.450 (1) | 0.117 (2) | 7.2 (5) |
| C(21) | 0.265 (2) | 0.563 (2) | 0.102 (2) | 8.1 (6) |
| C(22) | 0.191 (2) | 0.611 (2) | 0.023 (2) | 7.2 (5) |
| C(23) | 0.154 (2) | 0.554 (2) | −0.034 (2) | 8.0 (6) |
| C(24) | 0.210 (2) | 0.434 (2) | −0.015 (2) | 8.3 (6) |

[a] Values for anisotropically refined atoms are given in the form of the equivalent isotropic displacement parameter defined as $(4/3)[a^2\beta_{11} + b^2\beta_{22} + c^2\beta_{33} + ab(\cos\gamma)\beta_{12} + ac(\cos\beta)\beta_{13} + bc(\cos\alpha)\beta_{23}]$.

**Table VI.** Positional and Isotropic Equivalent Displacement Parameters[a] and Their Estimated Standard Deviations for $W_2Br_6(PMe_2Ph)_3$ (**4b**)

| atom | x | y | z | B, Å² |
|---|---|---|---|---|
| W(1) | 0.43644 (4) | 0.27019 (2) | 0.22099 (4) | 2.161 (8) |
| W(2) | 0.65752 (4) | 0.25277 (2) | 0.17737 (4) | 2.284 (8) |
| Br(1) | 0.5440 (1) | 0.40654 (6) | 0.2735 (1) | 3.28 (2) |
| Br(2) | 0.6115 (1) | 0.15340 (6) | 0.34291 (9) | 3.43 (2) |
| Br(3) | 0.4785 (1) | 0.20475 (7) | −0.02358 (9) | 3.34 (2) |
| Br(4) | 0.2767 (1) | 0.16615 (7) | 0.1927 (1) | 4.25 (2) |
| Br(5) | 0.8473 (1) | 0.28396 (8) | 0.3608 (1) | 4.60 (3) |
| Br(6) | 0.7174 (1) | 0.33412 (7) | 0.0119 (1) | 4.51 (2) |
| P(1) | 0.2648 (3) | 0.3655 (2) | 0.0742 (3) | 3.16 (5) |
| P(2) | 0.4090 (2) | 0.3137 (2) | 0.4676 (2) | 2.73 (5) |
| P(3) | 0.7788 (3) | 0.1121 (2) | 0.0889 (2) | 2.97 (5) |
| C(1) | 0.327 (1) | 0.4245 (8) | −0.032 (1) | 5.0 (3) |
| C(2) | 0.149 (1) | 0.3065 (8) | −0.048 (1) | 5.1 (3) |
| C(3) | 0.163 (1) | 0.4462 (7) | 0.170 (1) | 3.4 (2) |
| C(4) | 0.194 (1) | 0.5250 (7) | 0.212 (1) | 3.9 (2) |
| C(5) | 0.123 (1) | 0.5831 (8) | 0.294 (1) | 4.9 (3) |
| C(6) | 0.020 (1) | 0.5585 (9) | 0.331 (1) | 5.1 (3) |
| C(7) | −0.017 (1) | 0.4792 (9) | 0.289 (1) | 5.3 (3) |
| C(8) | 0.054 (1) | 0.4199 (8) | 0.206 (1) | 4.4 (3) |
| C(9) | 0.558 (1) | 0.3287 (7) | 0.586 (1) | 4.0 (2) |
| C(10) | 0.307 (1) | 0.4132 (7) | 0.502 (1) | 4.2 (3) |
| C(11) | 0.3410 (9) | 0.2366 (6) | 0.5331 (9) | 2.9 (2) |
| C(12) | 0.421 (1) | 0.1680 (8) | 0.6001 (9) | 3.9 (2) |
| C(13) | 0.367 (1) | 0.1077 (8) | 0.641 (1) | 4.9 (3) |
| C(14) | 0.238 (1) | 0.1081 (8) | 0.611 (1) | 4.7 (2) |
| C(15) | 0.155 (1) | 0.1740 (8) | 0.546 (1) | 4.7 (3) |
| C(16) | 0.206 (1) | 0.2360 (7) | 0.505 (1) | 3.6 (2) |
| C(17) | 0.940 (1) | 0.0822 (9) | 0.193 (1) | 5.3 (3) |
| C(18) | 0.702 (1) | 0.0186 (6) | 0.076 (1) | 4.4 (2) |
| C(19) | 0.8127 (9) | 0.1089 (6) | −0.0804 (9) | 3.0 (2) |
| C(20) | 0.912 (1) | 0.1533 (7) | −0.097 (1) | 4.3 (3) |
| C(21) | 0.938 (1) | 0.1531 (9) | −0.224 (1) | 5.3 (3) |
| C(22) | 0.866 (1) | 0.1145 (9) | −0.336 (1) | 5.1 (3) |
| C(23) | 0.767 (1) | 0.0694 (8) | −0.322 (1) | 4.1 (3) |
| C(24) | 0.741 (1) | 0.0672 (7) | −0.189 (1) | 3.8 (2) |

[a] Values for anisotropically refined atoms are given in the form of the equivalent isotropic displacement parameter defined as: $(4/3)[a^2\beta_{11} + b^2\beta_{22} + c^2\beta_{33} + ab(\cos\gamma)\beta_{12} + ac(\cos\beta)\beta_{13} + bc(\cos\alpha)\beta_{23}]$.

were obtained from a Patterson synthesis and used to start the refinement. The positions of all other atoms were located and refined by alternating difference Fourier maps and least squares cycles. Anisotropic thermal parameters were assigned to all atoms of the molecule. No disorder problem arose in the refinement of the structure. Hydrogen atoms were not included in the model. The final difference Fourier map showed several peaks (highest 2.2 e/Å³) around the central core. The final positional and thermal parameters are listed in Table V.

**Crystal Structure of 4b.** Three check reflections measured periodically showed no significant decay of the crystal. In the Patterson synthesis positions of tungsten, bromine, and phosphorus atoms were located, and the refinement of the structure went smoothly. The carbon atoms in the phosphine ligands were found and refined by alternating difference Fourier maps and least-squares cycles. All atoms were refined anisotropically. Hydrogen atoms were not included in the structure. In the final difference Fourier map there was no peak greater than 1 e/Å³. The final positional and thermal parameters for this structure are given in Table VI.

## Results

**Preparative Chemistry.** Compound **1** was prepared by reducing $WCl_4$ with 1 equiv of Na/Hg in toluene followed by the addition of 2 equiv of $PMe_2Ph$ ligand (eq 1). This compound can also

$$WCl_4 + Na/Hg + 2PMe_2Ph \xrightarrow{\text{toluene}} W_2Cl_6(PMe_2Ph)_4 \quad (1)$$

be prepared by using $NaB(C_2H_5)_3H$ as reducing agent instead of Na/Hg in a similar reaction. Actually, our goal had been to prepare the mononuclear $WCl_3(PMe_2Ph)_3$ compound by converting the dinuclear compound $W_2Cl_6(PMe_2Ph)_4$ in the presence of excess phosphine (eq 2). However, only **1** was obtained. By

$$WCl_4 + NaB(C_2H_5)_3H + 2PMe_2Ph \xrightarrow{\text{toluene}} W_2Cl_6(PMe_2Ph)_4$$

$$W_2Cl_6(PMe_2Ph)_4 + 2PMe_2Ph \xrightarrow{\text{toluene}} 2WCl_3(PMe_2Ph)_3 \quad (2)$$

using 1.5 equiv instead of 2 equiv of the phosphine ligand in eq 1 compound **2** was prepared. Bromo-bridged dinuclear complexes **4** and **5** were prepared by reducing $WBr_5$ with 2 equiv of reducing agent followed by the addition of 1.5 equiv of appropriate phosphine ligand. Attempts to prepare the corresponding edge-sharing compound, namely $W_2Br_6(PMe_2Ph)_4$ failed. For example, when compound **4** was heated at 60 °C for 2 h with one equiv of $PMe_2Ph$ and filtered through Celite followed by the layering with hexane, there was no chemical reaction (unit cell of these crystals was that of **4a**).

All complexes reported here are stable toward air in the solid state but then decompose or are converted to mononuclear oxo species in solution. When a solution of compound **4** was opened to air and left undisturbed, a second set of crystals of $WOBr_2(PMe_2Ph)_3$ was found. This oxo species was also formed as a byproduct in the initial preparation of **4** but very careful exclusion of oxygen prevented its formation.

Compounds **1**, **2**, and **4** (in two crystalline forms, **4a** and **4b**) were structurally characterized by X-ray diffraction methods. Electronic spectra and $^{31}P\{^1H\}$ NMR spectra for these complexes were also obtained. We will discuss the structure and bonding in these complexes first and then the spectroscopic results.

**Crystal Structures. Compound 1.** The crystal structure of **1** is shown in Figure 1. A crystallographic 2-fold axis of symmetry passes through the two metal centers, thus relating each of the unlabeled ligand atoms to one of the labeled ones. Table VII lists the selected bond distances and angles for **1**. Bending of the axial chlorine atoms on W(1) and phosphine ligands on W(2) resulted from the strong metal to metal interaction. The W–W distance is 2.6950 (3) Å. The terminal W–Cl axial bond length is 2.454 (1) Å, and the terminal W–Cl equatorial bond length is 2.399

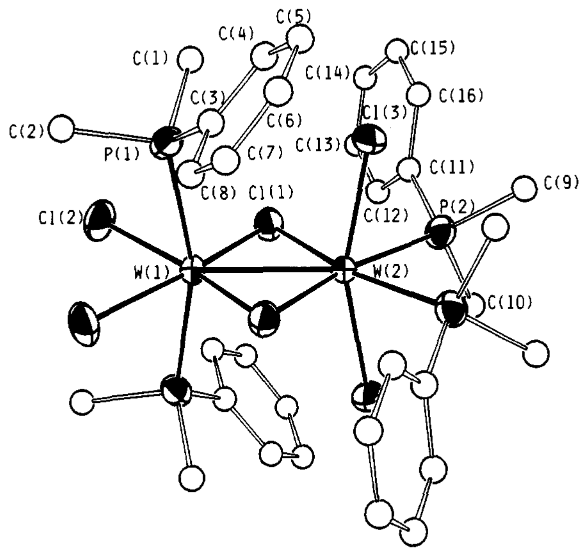


**Figure 1.** ORTEP drawing of the $W_2Cl_6(PMe_2Ph)_4$ molecule in **1**. Noncarbon atoms are drawn at the 50% probability level; carbon atoms are shown as spheres of arbitrarily small radius.

**Table VII.** Selected Bond Distances (Å) and Bond Angles (deg) for $W_2Cl_6(PMe_2Ph)_4$ (**1**)[a]

| | | | |
|---|---|---|---|
| W(1)–W(2) | 2.6950 (3) | W(2)–Cl(1) | 2.398 (1) |
| W(1)–Cl(1) | 2.361 (1) | W(2)–Cl(3) | 2.399 (1) |
| W(1)–Cl(2) | 2.454 (1) | W(2)–P(2) | 2.593 (1) |
| W(1)–P(1) | 2.552 (1) | | |
| W(2)–W(1)–Cl(1) | 56.15 (2) | W(1)–W(2)–Cl(3) | 100.67 (3) |
| W(2)–W(1)–Cl(2) | 136.76 (3) | W(1)–W(2)–P(2) | 134.07 (3) |
| W(2)–W(1)–P(1) | 98.35 (3) | Cl(1)–W(2)–Cl(1)′ | 109.75 (4) |
| Cl(1)–W(1)–Cl(1)′ | 112.30 (4) | Cl(1)–W(2)–Cl(3) | 102.20 (4) |
| Cl(1)–W(1)–Cl(2) | 80.93 (4) | Cl(1)′–W(2)–Cl(3) | 90.10 (4) |
| Cl(1)′–W(1)–Cl(2) | 165.76 (4) | Cl(1)–W(2)–P(2) | 79.27 (4) |
| Cl(1)–W(1)–P(1) | 90.32 (4) | Cl(1)′–W(2)–P(2) | 170.58 (3) |
| Cl(1)–W(1)–P(1) | 98.99 (4) | Cl(3)–W(2)–Cl(3)′ | 158.66 (4) |
| Cl(2)–W(1)–Cl(2)′ | 86.47 (4) | Cl(3)–W(2)–P(2) | 85.18 (4) |
| Cl(2)–W(1)–P(1) | 85.75 (4) | Cl(3)′–W(2)–P(2) | 80.01 (4) |
| Cl(2)′-W(1)-P(1) | 82.10 (4) | P(2)–W(2)–P(2)′ | 91.87 (4) |
| P(1)–W(1)–P(1)′ | 163.30 (4) | W(1)–Cl(1)–W(2) | 68.98 (3) |
| W(1)–W(2)–Cl(1) | 54.87 (2) | | |

[a] Numbers in parentheses are estimated standard deviations in the least significant digits.

(1) Å. The average bridging W–Cl bond distance, 2.379 [2] Å, is slightly shorter than the terminal W–Cl axial or equatorial bond lengths. The W–P equatorial distances are slightly longer than the W–P axial distances. The W–$Cl_b$–W angle is 68.98 (3)°. The eight atoms of the central plane show no deviation greater than 0.07 Å from the mean plane, and the plane defined by the metal atoms and the four axial atoms makes an angle of 88.71 (3)° with the equatorial plane.

**Compound 2.** An ORTEP drawing of compound **2** is shown in Figure 2. It has the confacial bioctahedral geometry with the anti configuration of the terminal ligands. The molecule does not have any crystallographically imposed symmetry, but the core has an effective plane of symmetry which passes through two tungsten atoms, the terminal Cl(4) atom, the P(3) atom, and the bridging Cl(1) atom. Selected bond distances and angles for this structure are given in Table VIII. The W–W distance of 2.4433 (4) Å indicates that a strong metal–metal bond is present. The average W–$Cl_b$–W bond angle is 58.45 [4]°. The average W–Cl terminal distance is shorter by ca. 0.14 Å than the average W–Cl bridging distance. The average W–P bond length is 2.537 [2] Å.

**Compounds 4a and 4b.** ORTEP drawings of the molecules in **4a** and **4b** are shown in Figures 3 and 4, respectively. Crystallographically **4a** and **4b** are different but chemically they are the same. Principal bond distances and angles for **4a** and **4b** are listed in Table IX. Both structures contain molecules with face-sharing bioctahedral geometry and an anti configuration of the terminal ligands. Each of them has a $W_2Br_6P_3$ core with an effective plane of symmetry which passes through the W(1), W(2), Br(4), P(3),

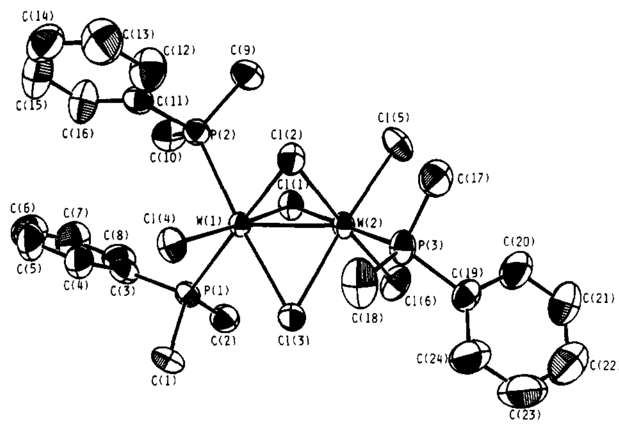


**Figure 2.** An ORTEP drawing of $W_2Cl_6(PMe_2Ph)_3$ in **2**. Atoms are drawn at the 50% probability level.

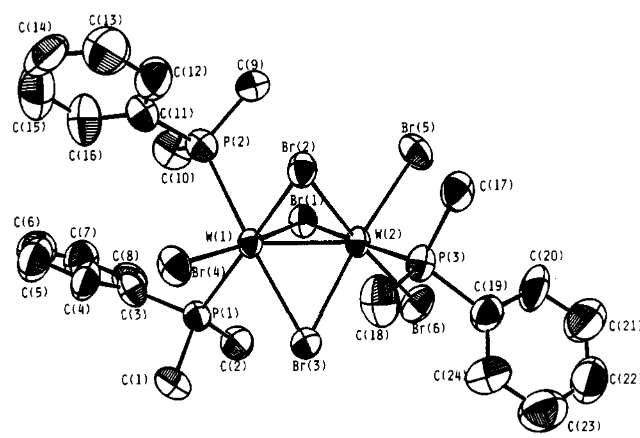


**Figure 3.** ORTEP drawing of $W_2Br_6(PMe_2Ph)_3$ in **4a**. Atoms are drawn at the 50% probability level.

**Table VIII.** Selected Bond Distances (Å) and Bond Angles (deg) for $W_2Cl_6(PMe_2Ph)_3$ (**2**)[a]

| | | | |
|---|---|---|---|
| W(1)–W(2) | 2.4433 (4) | W(2)–Cl(1) | 2.530 (2) |
| W(1)–Cl(1) | 2.460 (2) | W(2)–Cl(2) | 2.500 (2) |
| W(1)–Cl(2) | 2.511 (2) | W(2)–Cl(3) | 2.484 (2) |
| W(1)–Cl(3) | 2.527 (2) | W(2)–Cl(5) | 2.367 (2) |
| W(1)–Cl(4) | 2.375 (2) | W(2)–Cl(6) | 2.358 (2) |
| W(1)–P(1) | 2.541 (2) | W(2)–P(3) | 2.523 (2) |
| W(1)–P(2) | 2.546 (2) | | |
| W(2)–W(1)–Cl(1) | 62.11 (4) | W(1)–W(2)–Cl(3) | 61.70 (4) |
| W(2)–W(1)–Cl(2) | 60.59 (4) | W(1)–W(2)–Cl(5) | 122.63 (5) |
| W(2)–W(1)–Cl(3) | 59.93 (5) | W(1)–W(2)–Cl(6) | 123.66 (6) |
| W(2)–W(1)–Cl(4) | 127.22 (5) | W(1)–W(2)–P(3) | 121.02 (5) |
| W(2)–W(1)–P(1) | 121.60 (4) | Cl(1)–W(2)–Cl(2) | 100.21 (5) |
| W(2)–W(1)–P(2) | 116.05 (5) | Cl(1)–W(2)–Cl(3) | 97.38 (6) |
| Cl(1)–W(1)–Cl(2) | 101.84 (7) | Cl(1)–W(2)–Cl(5) | 86.90 (6) |
| Cl(1)–W(1)–Cl(3) | 98.07 (6) | Cl(1)–W(2)–Cl(6) | 84.14 (6) |
| Cl(1)–W(1)–Cl(4) | 170.61 (7) | Cl(1)–W(2)–P(3) | 179.47 (7) |
| Cl(1)–W(1)–P(1) | 85.73 (6) | Cl(2)–W(2)–Cl(3) | 96.41 (6) |
| Cl(1)–W(1)–P(2) | 79.13 (6) | Cl(2)–W(2)–Cl(5) | 84.78 (7) |
| Cl(2)–W(1)–Cl(3) | 95.04 (6) | Cl(2)–W(2)–Cl(6) | 175.06 (7) |
| Cl(2)–W(1)–Cl(4) | 85.28 (7) | Cl(2)–W(2)–P(3) | 79.66 (6) |
| Cl(2)–W(1)–P(1) | 171.72 (6) | Cl(3)–W(2)–Cl(5) | 175.26 (6) |
| Cl(2)–W(1)–P(2) | 82.78 (6) | Cl(3)–W(2)–Cl(6) | 85.28 (7) |
| Cl(3)–W(1)–Cl(4) | 87.27 (6) | Cl(3)–W(2)–P(3) | 83.15 (7) |
| Cl(3)–W(1)–P(1) | 80.44 (6) | Cl(5)–W(2)–Cl(6) | 93.17 (8) |
| Cl(3)–W(1)–P(2) | 175.97 (7) | Cl(5)–W(2)–P(3) | 92.57 (7) |
| Cl(4)–W(1)–P(1) | 87.57 (7) | Cl(6)–W(2)–P(3) | 95.97 (6) |
| Cl(4)–W(1)–P(2) | 95.89 (6) | W(1)–Cl(1)–W(2) | 58.61 (4) |
| P(1)–W(1)–P(2) | 102.14 (6) | W(1)–Cl(2)–W(2) | 58.38 (4) |
| W(1)–W(2)–Cl(1) | 59.27 (4) | W(1)–Cl(3)–W(2) | 58.36 (4) |
| W(1)–W(2)–Cl(2) | 61.04 (5) | | |

[a] Numbers in parentheses are estimated standard deviations in the least significant digits.

**Table IX.** Selected Bond Distances (Å) and Bond Angles (deg) for **4a** and **4b**[a]

| | **4a** | **4b** |
|---|---|---|
| | Bond Distances | |
| W(1)-W(2) | 2.4768 (9) | 2.4496 (6) |
| W(1)-Br(1) | 2.582 (2) | 2.580 (1) |
| W(1)-Br(2) | 2.638 (2) | 2.645 (1) |
| W(1)-Br(3) | 2.644 (1) | 2.651 (1) |
| W(1)-Br(4) | 2.527 (2) | 2.532 (1) |
| W(1)-P(1) | 2.556 (4) | 2.538 (2) |
| W(1)-P(2) | 2.605 (3) | 2.565 (2) |
| W(2)-Br(1) | 2.647 (1) | 2.692 (1) |
| W(2)-Br(2) | 2.631 (1) | 2.639 (1) |
| W(2)-Br(3) | 2.611 (2) | 2.619 (1) |
| W(2)-Br(5) | 2.522 (2) | 2.519 (1) |
| W(2)-Br(6) | 2.527 (2) | 2.506 (1) |
| W(2)-P(3) | 2.540 (3) | 2.538 (2) |
| | Bond Angles | |
| W(2)-W(1)-Br(1) | 63.05 (4) | 64.66 (3) |
| W(2)-W(1)-Br(2) | 61.82 (4) | 62.27 (3) |
| W(2)-W(1)-Br(3) | 61.21 (4) | 61.64 (3) |
| W(2)-W(1)-Br(4) | 128.35 (4) | 132.11 (3) |
| W(2)-W(1)-P(1) | 122.27 (8) | 116.45 (7) |
| W(2)-W(1)-P(2) | 116.2 (1) | 116.43 (6) |
| Br(1)-W(1)-Br(2) | 103.35 (5) | 104.27 (3) |
| Br(1)-W(1)-Br(3) | 99.31 (5) | 104.85 (4) |
| Br(1)-W(1)-Br(4) | 168.58 (5) | 163.22 (4) |
| Br(1)-W(1)-P(1) | 85.37 (9) | 81.73 (6) |
| Br(1)-W(1)-P(2) | 79.89 (6) | 79.0 (1) |
| Br(2)-W(1)-Br(3) | 96.67 (5) | 93.23 (3) |
| Br(2)-W(1)-Br(4) | 84.81 (6) | 86.98 (4) |
| Br(2)-W(1)-P(1) | 171.11 (9) | 171.51 (6) |
| Br(2)-W(1)-P(2) | 81.79 (9) | 79.62 (5) |
| Br(3)-W(1)-Br(4) | 87.50 (5) | 86.58 (4) |
| Br(3)-W(1)-P(1) | 79.99 (8) | 79.28 (6) |
| Br(3)-W(1)-P(2) | 177.4 (1) | 172.31 (6) |
| Br(4)-W(1)-P(1) | 86.81 (9) | 88.55 (7) |
| Br(4)-W(1)-P(2) | 94.5 (1) | 90.18 (7) |
| P(1)-W(1)-P(2) | 101.8 (1) | 107.63 (8) |
| W(1)-W(2)-Br(1) | 60.42 (4) | 60.02 (3) |
| W(1)-W(2)-Br(2) | 62.10 (4) | 62.50 (3) |
| W(1)-W(2)-Br(3) | 62.56 (4) | 62.96 (3) |
| W(1)-W(2)-Br(5) | 123.24 (4) | 122.30 (4) |
| W(1)-W(2)-Br(6) | 124.16 (5) | 122.33 (4) |
| W(1)-W(2)-P(3) | 121.83 (9) | 123.87 (7) |
| Br(1)-W(2)-Br(2) | 101.78 (4) | 101.37 (4) |
| Br(1)-W(2)-Br(3) | 98.50 (5) | 102.62 (3) |
| Br(1)-W(2)-Br(5) | 86.20 (5) | 84.05 (4) |
| Br(1)-W(2)-Br(6) | 83.49 (5) | 84.50 (4) |
| Br(1)-W(2)-P(3) | 177.7 (1) | 176.08 (7) |
| Br(2)-W(2)-Br(3) | 97.66 (5) | 94.10 (4) |
| Br(2)-W(2)-Br(5) | 84.86 (5) | 85.48 (4) |
| Br(2)-W(2)-Br(6) | 173.59 (6) | 174.00 (4) |
| Br(2)-W(2)-P(3) | 79.38 (8) | 80.86 (7) |
| Br(3)-W(2)-Br(5) | 174.06 (5) | 173.25 (4) |
| Br(3)-W(2)-Br(6) | 85.04 (6) | 85.73 (4) |
| Br(3)-W(2)-P(3) | 83.3 (1) | 80.34 (6) |
| Br(5)-W(2)-Br(6) | 91.92 (6) | 93.99 (4) |
| Br(5)-W(2)-P(3) | 91.9 (1) | 92.94 (6) |
| Br(6)-W(2)-P(3) | 95.23 (8) | 93.21 (7) |
| W(1)-Br(1)-W(2) | 56.53 (3) | 55.32 (2) |
| W(1)-Br(2)-W(2) | 56.08 (3) | 55.24 (2) |
| W(1)-Br(3)-W(2) | 56.23 (3) | 55.39 (2) |

[a] Numbers in parentheses are estimated standard deviation in the least significant digits.

and Br(1) atoms. The W–W bond distances are 2.4768 (9) and 2.4496 (6) Å for **4a** and **4b**, respectively. The average W–Br bridging bond lengths are 2.626 [2] (for **4a**) and 2.638 [1] Å (for **4b**) and the average W–Br terminal distances are 2.525 [2] and 2.519 [1] Å for **4a** and **4b**, respectively. The average W–P bond distances are 2.567 [3] and 2.547 [2] Å for **4a** and **4b**, respectively. The average W–$Br_b$–W bond angles are 56.28 [3] and 55.32 [2]° for **4a** and **4b**, respectively.

The difference between the $W_2Br_6(PMe_2Ph)_3$ molecules in **4a** and **4b** can be seen in Figures 3 and 4, and a few of the angular parameters are compared numerically in Table X. They differ in the orientations of the $PMe_2Ph$ ligands, which gives them different shapes. Given that they have different shapes, it is understandable that they pack differently, thus making their crystals different. The two packings are shown in Figures 5 and 6. As expected from the unit cell volumes, **4b** is more closely packed than **4a**. However, it could as easily, and as correctly, be said that because the crystal packing is different in **4a** and **4b**, the molecules take on different shapes. We simply do not know what factor is responsible for the initiation of growth of one form or the other. They presumably differ very little in stability,

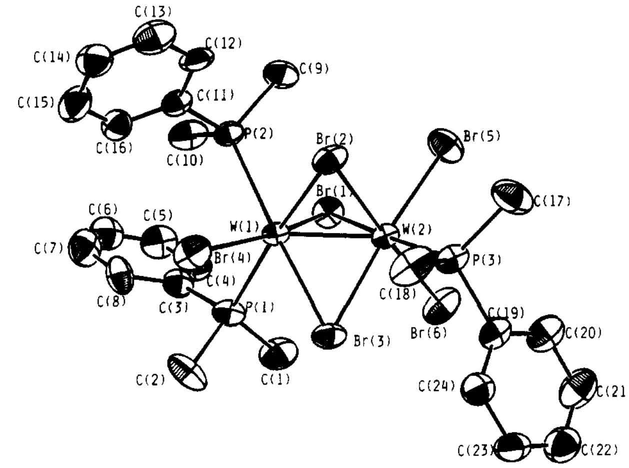


**Figure 4.** An ORTEP drawing of $W_2Br_6(PMe_2Ph)_3$ in **4b**. Atoms are drawn at the 50% probability level.

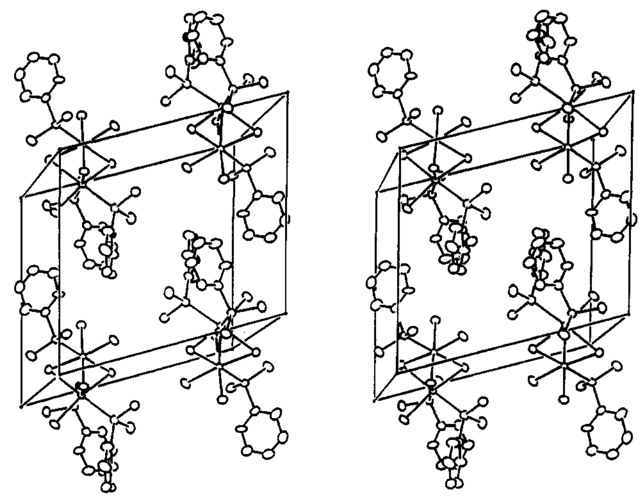

**Figure 5.** Unit cell diagrams of $W_2Br_6(PMe_2Ph)_3$ in **4a**. Axes orientation: *c*, down; *a*, across; *b*, toward viewer. Atoms are represented by their thermal ellipsoids at the 20% probability level.

**Table X.** Comparison of Selected Torsional Angles (deg) and Dihedral Angles (deg) between the Planes for **4a** and **4b**[a]

Torsional Angles

| atoms | angle **4a** | angle **4b** |
|---|---|---|
| C(3)-P(1)-W(1)-W(2) | −149.2 (5) | −130.7 (4) |
| C(11)-P(2)-W(1)-W(2) | −127.4 (6) | −119.9 (4) |
| C(19)-P(3)-W(2)-W(1) | 137.8 (5) | 113.5 (4) |

Dihedral Angles

| planes | angle **4a** | angle **4b** |
|---|---|---|
| C(3)-P(1)-W(1)/C(4)-C(3)-C(8) | 68.9 (11) | 86.2 (7) |
| C(11)-P(2)-W(1)/C(12)-C(11)-C(16) | 102.9 (10) | 94.6 (6) |
| C(19)-P(3)-W(2)/C(20)-C(19)-C(24) | 104.9 (8) | 75.4 (6) |

[a] Numbers in parentheses are estimated standard deviations in the least significant digits.

**Table XI.** Comparison of Dimensions in $M_2X_6L_4$ and $M_2X_6L_3$ Complexes, Where M = Mo or W, X = Cl or Br, and L = Monodentate Nitrogen or Phosphorus Ligand[a]

$M_2X_6L_4$ Complexes

| compound | type of bond, Å | | | | | | angle, deg | ref |
|---|---|---|---|---|---|---|---|---|
| | M-M | $M-X_a$ | $M-X_e$ | $M-X_b$ | $M-L_a$ | $M-L_e$ | $M-X_b-M$ | |
| $W_2Cl_6(PMe_3)_4$ | 2.7113 (8) | 2.413 [2] | 2.462 [2] | 2.394 [2] | 2.526 [3] | 2.568 [3] | 68.98 [7] | 16 |
| $W_2Cl_6(PEt_3)_4$ | 2.7397 (7) | 2.407 [2] | 2.453 [2] | 2.396 [2] | 2.564 [3] | 2.606 [3] | 69.74 [6] | 7, 16 |
| $W_2Cl_6(PMe_2Ph)_4$ | 2.6950 (3) | 2.399 (1) | 2.454 (1) | 2.379 [2] | 2.552 [1] | 2.593 (1) | 68.98 (3) | this work |
| $W_2Cl_6(Py)_4$ | 2.737 (3) | 2.397 (8) | 2.430 (8) | 2.392 [7] | 2.18 (2) | 2.24 (2) | 69.8 (2) | 17 |
| $Mo_2Cl_6(PEt_3)_4$ | 3.730 (1) | 2.384 (3) | 2.375 (5) | 2.501 [4] | 2.596 (3) | 2.545 [5] | 96.4 (1) | 4 |
| $Mo_2Cl_6(PMe_2Ph)_4{\cdot}2CHCl_3$ | 2.8036 (8) | 2.398 [1] | 2.441 [1] | 2.401 [1] | 2.576 [1] | 2.583 [1] | 71.45 [4] | 6 |

$M_2X_6L_3$ Complexes

| compound | type of bond, Å | | | | angle, deg | ref |
|---|---|---|---|---|---|---|
| | M-M | $M-X_t$ | $M-X_b$ | M-L | $M-X_b-M$ | |
| $W_2Cl_6(PEt_3)_3{\cdot}CH_2Cl_2$ | 2.4705 (7) | 2.383 [3] | 2.492 [3] | 2.547 [3] | 59.41 [7] | 7, 16 |
| $W_2Cl_6(PMe_2Ph)_3$ | 2.4433 (4) | 2.367 [2] | 2.502 [2] | 2.537 [2] | 58.45 [4] | this work |
| $W_2Br_6(PMe_2Ph)_3$ | 2.4768 (9) | 2.525 [2] | 2.626 [2] | 2.567 [3] | 56.28 [3] | this work |
| | 2.4496 (6) | 2.519 [1] | 2.638 [1] | 2.547 [2] | 55.32 [2] | |
| $Mo_2Cl_6(PEt_3)_3$ | 2.815 (4) | 2.36 [1] | 2.455 [8] | 2.57 [1] | 70.0 [2] | 5 |
| $Mo_2Cl_6(PEt_3)_3{\cdot}CH_2Cl_2$ | 2.753 (2) | 2.376 [4] | 2.470 [4] | 2.557 [4] | 67.7 [1] | 6 |
| $Mo_2Cl_6(PMe_2Ph)_3$ | 2.6582 (5) | 2.371 [1] | 2.479 [1] | 2.552 [1] | 64.83 [3] | 6 |

[a] Key: a = axial, e = equatorial, b = bridging, and t = terminal. Two different values in the same column indicate that this compound exists in two different crystalline forms.

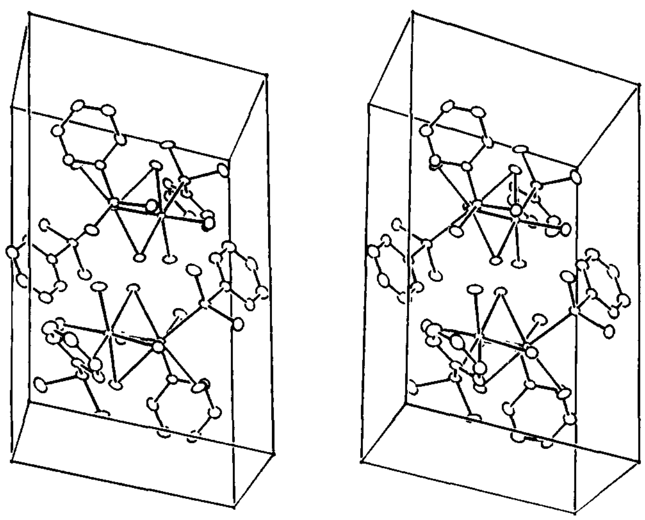

**Figure 6.** Unit cell diagrams of $W_2Br_6(PMe_2Ph)_3$ in **4b**. Axes orientation: 4c, down; *a*, across; *b*, toward viewer. Atoms are represented by their thermal ellipsoids at the 20% probability level.

although **4a** may be the more stable since it is more frequently formed.

**NMR Spectra.** The $^{31}P\{^1H\}$ NMR spectrum of **3** consists of a doublet at $\delta = -33.71$ ppm and a triplet at $\delta = 20.84$ ppm in the intensity ratio 2:1 corresponding to two phosphorus atoms on one tungsten atom and to a single phosphorus atom on the other tungsten atom. Tungsten satellites are also observed due to tungsten to phosphorus couplings ($^{183}W$ has nuclear spin of $^1/_2$ and a natural abundance of 14%); the $^1J_{P-W}$ and $^2J_{P-W}$ values for the doublet are 254.5 and 173.7 Hz, respectively and $^1J_{P-W}$ for the triplet is 198.8 Hz. The $^2J_{P-P}$ coupling constant is 44.7 Hz.

The electronic spectra of **1**, **4**, and **5** are shown in Figure 7. The spectrum of **1** consists of two peaks at 670 and 460 nm and a shoulder at 370 nm. The spectrum of **5** is very similar to that of **4** and indicates that they have similar structures in solution.

## Discussion

We have found that $WCl_4$ and $WBr_5$ are very good starting materials for the syntheses of edge-sharing and face-sharing chloro-bridged and bromo-bridged dinuclear complexes of W(III), respectively. In each reaction the formation of W(III) species from W(IV) or W(V) halides by employing the appropriate amount of reducing agent in toluene is the first step, and then the very reactive W(III) species forms the dinuclear phosphine complex, edge-sharing or face-sharing, depending on the amount of the phosphine ligand added to it. Two different reducing agents, namely Na/Hg and $NaB(C_2H_5)_3H$, have been employed for this purpose. The use of Na/Hg to reduce $WCl_4$ for the preparation of a dinuclear W(III) compound, $W_2Cl_6(PMe_3)_4$, has been reported[14] before but not in hydrocarbon solvents. On the other hand, other tungsten(III) dinuclear phosphine complexes reported by Chisholm et al.[7] were only indirectly prepared from $WCl_4$, by way of an isolated W(III) intermediate. Therefore, the new synthetic routes reported here are simpler and more straightforward than earlier ones.

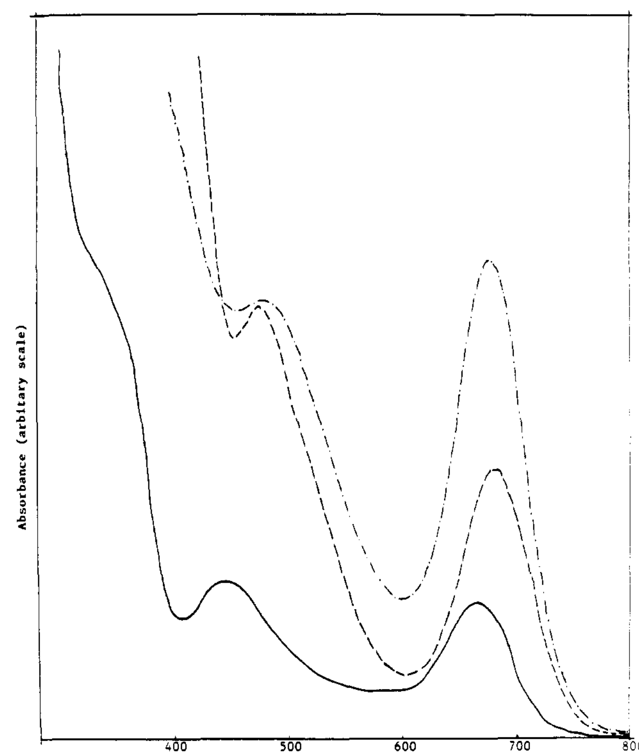


**Figure 7.** Electronic spectra of **1** (—), **4a** (--) and **5** (-·-) in toluene.

(14) (a) Sharp, P. R.; Schrock, R. R. *J. Am. Chem. Soc.* **1980**, *102*, 1430. (b) Schrock, R. R.; Sturgeoff, L. G.; Sharp, P. R. *Inorg. Chem.* **1983**, *22*, 1801.

Our attempt to prepare the mononuclear species $WCl_3(PMe_2Ph)_3$ from the dinuclear edge-sharing compound $W_2Cl_6(PMe_2Ph)_4$ in the presence of excess phosphine ligand was unsuccessful. Recently, it was reported[15] that the opposite reaction does not proceed either. We find this result puzzling and are reexamining it.

We carried out the $^{31}P$ NMR experiment for **1** to determine whether we could observe an equilibrium between the edge-sharing and face-sharing dinuclear complexes as reported[7] by Chisholm et al. for the $PEt_3$ ligand. We have not yet been able to observe such an equilibrium, but the work is continuing. The $^{31}P\{^1H\}$ NMR spectrum of **3** is similar to that of the face-sharing compound[7] $W_2Cl_6(PEt_3)_3$ (**6**) in equilibrium with the corresponding edge-sharing compound, and the $^2J_{P-P}$ values are 44.7 and 44.0 Hz for **3** and **6**, respectively.

The crystal structures of these complexes allow us to make some interesting comparisons with those of related molybdenum and tungsten compounds, as shown in Table XI. The W-W bond lengths in compounds **2** and **4b** are the shortest in any neutral halogen-bridged dinuclear W(III) complexes so far reported. Another striking feature in the bromo-bridged complexes **4a** and **4b** is that the average $W-Br_b-W$ angles are only 56.28 (for **4a**) and 55.32° (for **4b**). In general, the $M-X_b$ distances are shorter than the $M-X_t$ distances in the edge-sharing compounds while the opposite is true in the face-sharing compounds.

**Acknowledgment.** We thank Professor M. H. Chisholm for providing unpublished information and Dr. Lee M. Daniels for very helpful discussion and aid with graphics. We also thank the Robert A. Welch Foundation for financial support.

**Registry No.** 1, 139376-26-4; 2, 139376-27-5; 3, 139376-28-6; 4a, 139376-29-7; 5, 139376-30-0; W, 7440-33-7.

**Supplementary Material Available:** Full tables of hydrogen atom parameters, bond distances, bond angles, and anisotropic displacement parameters for **1**, **2**, **4a**, and **4b** and a least-squares planes for **1** (26 pages); tables of observed and calculated structure factors for **1**, **2**, **4a**, and **4b** (81 pages). Ordering information is given on any current masthead page.

(15) Hills, A.; Hughes, D. L.; Leigh, G. L.; Prieto-Alcon, R. *J. Chem. Soc., Dalton Trans.* **1991**, 1515.
(16) Chisholm, M. H. Private communications, 1991.
(17) Jackson, R. B.; Strieb, W. E. *Inorg. Chem.* **1971**, *10*, 1760.

Contribution from the Department of Chemistry, The University of Calgary, Calgary, Alberta, Canada T2N 1N4

# Reactions of $Ph_2PN_2(SiMe_3)_3$ with Organochalcogen Halides: Preparation, X-ray Structure, and Reactions of $Ph_2PN_2(SiMe_3)_2(SPh)$ with $E_2Cl_2$ (E = S, Se) and PhSeCl

Tristram Chivers,* Santhanathan S. Kumaravel, Masood Parvez, and M. N. Sudheendra Rao

*Received October 15, 1991*

The reactions of $Ph_2PN_2(SiMe_3)_3$ with arenesulfenyl chlorides in a 1:1 or 1:3 molar ratio in methylene dichloride produces the metathetical products $Ph_2PN_2(SiMe_3)_2(SAr)$ [**1a**, Ar = Ph; **1b**, Ar = 2,4-$(NO_2)_2C_6H_3$] or $Ph_2PN_2(SAr)_3$ (**2d**, Ar = 2,4-$(NO_2)_2C_6H_3$), respectively. Compound **2d** is thermally stable below ca. 80 °C whereas the trisubstituted derivatives $Ph_2PN_2(EPh)_3$ (E = S, Se) decompose above 0 °C to give the eight-membered rings 1,5-$Ph_4P_2N_4E_2Ph_2$ with the elimination of $Ph_2E_2$. The structure of **1a** was determined by X-ray crystallography. The crystals of **1a** are monoclinic, space group $P2_1$ with $a$ = 9.824 (4) Å, $b$ = 10.322 (3) Å, $c$ = 13.425 (7) Å, $\beta$ = 102.75 (4)°, $V$ = 1327.8 Å$^3$, and $Z$ = 2. The three-coordinate (amino) nitrogen atom in **1a** is attached to three consecutive third-row elements (Si, P, and S). The reaction of **1a** with 2 molar equiv of PhSeCl or with $Se_2Cl_2$ produces 1,5-$Ph_4P_2N_4S_2Ph_2$ in 65–75% with the elimination of $Ph_2Se_2$ and selenium, respectively. The reactions of **1a** or $Ph_2PN_2(SiMe_3)_3$ with $S_2Cl_2$ under a variety of conditions yield the heterocycles 1,5-$Ph_4P_2N_4S_2Cl_2$ and $Ph_4P_2N_3SCl$ as the major products.

## Introduction

The readily prepared reagents $R_2PN_2(SiMe_3)_3$[1] provide a fertile source of eight-membered phosphorus–nitrogen (P–N) ring systems containing sulfur or selenium in a low oxidation state (see Scheme I).[2-5] These cyclocondensation reactions with polyfunctional reagents must involve a number of steps. In an attempt to gain a better understanding of these systems, we have investigated the reactions of $R_2PN_2(SiMe_3)_3$ (R = Ph, Me) with *mono*functional reagents of the type PhECl (E = S, Se). When these reactions are carried out in a 1:3 molar ratio (eq 1) the eight-membered rings 1,5-$Ph_4P_2N_4E_2Ph_2$ are obtained in good yields, with the elimination of $Ph_2E_2$, as described in a preliminary communication.[6]

In this account we provide further details of these investigations, including (a) the preparation of the monosubstituted derivatives $R_2PN_2(SiMe_3)_2(SAr)$ (**1a**, R = Ar = Ph; **1b**, R = Ph, Ar = 2,4-$C_6H_3(NO_2)_2$; **1c**, R = Me, Ar = Ph), (b) the X-ray structure of **1a**, (c) the preparation of the trisubstituted derivative $Ph_2PN_2(SAr)_3$ [Ar = 2,4-$C_6H_3(NO_2)_2$], (d) the formation of the eight-membered rings 1,5-$R_4P_2N_4E_2Ph_2$ (R = Me, Ph, E = S; R = Ph, E = Se) by the decomposition of $R_2PN_2(EPh)_3$; (e) the preparation of 1,5-$Ph_4P_2N_4S_2Ph_2$ by the reaction of **1a** with PhSeCl (1:2 molar ratio) or $Se_2Cl_2$, and (f) the reactions of **1a** or $Ph_2PN_2(SiMe_3)_3$ with $S_2Cl_2$.

**Scheme I.** Preparation of $P_2N_4E_2$ Rings (E = S, Se) from $Ph_2PN_2(SiMe_3)_3$: (i) $SCl_2$[2] or $SOCl_2$;[3] (ii) $RSeCl_3$ (R = Me, Et, Ph);[4] (iii) $^4/_6SeCl_4$ + $^1/_6Se_2Cl_2$[5]

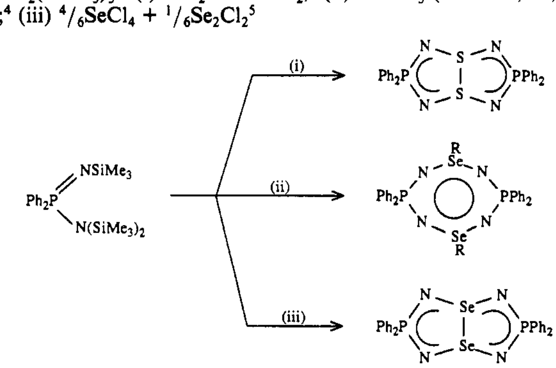


(1) (a) Wilburn, J. C.; Neilson, R. H. *Inorg. Chem.* **1977**, *16*, 2519. (b) Wilburn, J. C.; Wisian-Neilson, P.; Neilson, R. H. *Inorg. Chem.* **1979**, *18*, 1429.
(2) Chivers, T.; Dhathathreyan, K. S.; Liblong, S. W.; Parks, T. *Inorg. Chem.* **1988**, *27*, 1305.
(3) Chivers, T.; Edwards, M.; Parvez, M. *Inorg. Chem.*, in press.
(4) Chivers, T.; Doxsee, D. D.; Fait, J. F. *J. Chem. Soc., Chem. Commun.* **1989**, 1703.
(5) Chivers, T.; Doxsee, D. D. Unpublished observations.
(6) Chivers, T.; Kumaravel, S. S.; Meetsma, A.; van de Grampel, J. C.; van der Lee, A. *Inorg. Chem.* **1990**, *29*, 4591.

 